Oil Shale, 2020, Vol. 37, No. 4, pp. 288–303
doi: https://doi.org/10.3176/oil.2020.4.03
ISSN 0208-189X

Vapor pressures of narrow gasoline fractions of oil from industrial retorting of Kukersite oil shale

Parsa Mozaffari, Zachariah Steven Baird, Madis Listak, Vahur Oja*

Department of Energy Technology, School of Engineering, Tallinn University of Technology, Ehitajate tee 5, 19086 Tallinn, Estonia

Abstract. *This study presents vapor pressure data for narrow boiling range fractions, viewed as pseudocomponents, prepared by rectification from a wide Kukersite oil shale retort oil gasoline fraction, a straight-run fraction with a boiling range from about 40 to about 200 °C. This technical gasoline fraction was produced in a commercial solid heat carrier retort. Vapor pressures were measured according to the ASTM D6378 standard with a commercial ERAVAP vapor pressure tester using a vapor-liquid ratio of 4:1. The vapor pressure curves were derived by fitting the experimental data using the integrated form of the Clausius-Clapeyron equation. From this equation heats of vaporization and atmospheric boiling points were calculated. The suitability of three easy-to-use conventional oil vapor pressure correlations for predicting the vapor pressure of narrow boiling range fractions of Kukersite oil shale retort oil gasoline was evaluated.*

Keywords**:** *Kukersite oil shale, oil shale retort oil, gasoline fraction, pseudocomponents, vapor pressure, vapor pressure correlations.*

1. Introduction

Vaporization properties are important to be taken into account in transporting, handling and storing liquid oil products or evaluating their environmental risks [1–3]. This information can be used in calculations for designing processes and equipment and in modelling the spread of oil in the environment. For conventional oils, vapor pressure correlations are available for predicting vapor pressures from the basic properties of oils [4–7]. However, there is less information available for alternative oils, including oils produced via retorting (or pyrolysis) from oil shales from various deposits [8–11]. Many of these alternative oils contain polar compounds, which can make prediction more difficult due to the increased complexity of the intermolecular interactions in these oils [12–17].

* Corresponding author: e-mail *vahur.keemteh@outlook.com*

In general, our literature review indicated that only a small amount of data existed on the thermodynamic and transport properties of oils produced via retorting from oil shales, especially for their narrow boiling range fractions [18, 19]. For example, Estonian Kukersite oil shale retort oil is one of the most extensively studied oils of this type [12, 20, 21], but only limited information can be found in the literature [18, 19, 22–24]. A recent literature review by Oja et al. [19] on the thermodynamic properties of Kukersite oil shale retort oil showed that the publicly available information was spotty and poorly suitable for evaluating the applicability of the existing thermodynamic property prediction methods, even for evaluating the simplest approaches based on "undefined" pseudocomponents [5, 6]. Concerning the vaporization characteristics of Kukersite oil shale retort oil, Kollerov [18] presented data on the vapor pressures at different vapor-liquid ratios, including for some samples in the boiling range of gasoline and diesel. Also, data for a few narrow boiling range gasoline fractions were provided by Siitsman and Oja [16, 25]. At the same time, the studies by Siitsman et al. [26] and Astra and Oja [27] were focused only on evaluating the applicability of a differential scanning calorimetry method to measuring the vapor pressures of complex mixtures such as narrow boiling range oil fractions, while no vapor pressure data for the Kukersite straight-run gasoline sample was presented. It should be noted that in practice, there are various techniques for measuring the vapor pressure of oil-like compounds and complex mixtures depending on the volatility of the sample [28–33]. In the current study, the vapor pressures of the gasoline samples (narrow boiling fractions with boiling points of about 60 to 130 °C) were measured according to the ASTM D6378-10 standard [34], using a commercial ERAVAP analyzer (Eralytics GmbH, Vienna, Austria).

The purpose of this study was to provide the vapor pressure data for the Kukersite gasoline narrow boiling range fractions (distillation cuts that can be viewed as pseudocomponents). This information can be used for calculations related to handling, storage and risk assessment. Also, the applicability of the existing petroleum based easy-to-use vapor pressure correlations for these Kukersite gasoline fractions was evaluated [6, 35–38]. Lighter (i.e. lower boiling) fractions of Kukersite oil are known to contain more olefins and aromatic hydrocarbons than those of conventional oils [12, 19].

2. Experimental and methods

2.1. Sample preparation

The Kukersite oil shale gasoline fraction, a wide straight-run fraction with a boiling range from about 40 to about 200 °C, was obtained from Eesti Energia's Narva Oil Plant (Narva, Estonia). The plant uses solid heat carrier technology to convert oil shale organic matter into oil [39, 40]. In this

technology, pyrolysis vapors are fed from a retort to a distillation/separation column that separates oil into three broad industrial fractions: gasoline, fuel oil and heavy oil. The wide straight-run gasoline fraction used in the current study had a density of 0.7904 g/cm^3 and a refractive index of 1.4445 at 20 °C. Literature-based elemental composition data show that usually up to 3% of the Kukersite straight-run gasoline fractions consist of heteroatoms, most of which are likely sulfur and oxygen compounds [12, 13].

The wide straight-run gasoline fraction was further separated into fractions with narrow boiling ranges using rectification in accordance with ASTM D2892 [41]. For rectification, a packed distillation column with 24 theoretical plates and a 6:1 reflux ratio was used. The rectification was largely by volume, collecting approximately 18 to 20 ml of sample. During sample collection, the vapors were condensed in a glass condenser at about –10 °C and the liquid gasoline was then collected in pre-cooled vials (to about –10 °C) to ensure no loss of volatiles.

2.2. Vapor pressure measurements and data analysis

Vapor pressure was measured according to ASTM D6378-10 [34] with said ERAVAP analyzer using a vapor-liquid ratio of 4:1. The instrument had a temperature range of 273–393 K and a pressure range from a few kPa to 1000 kPa. Based on experience, the device was best suited for samples with vapor pressures between 10 and 150 kPa at 310.95 K. The accuracy of the measurements made with the apparatus was checked by measuring the vapor pressure of benzene between 40 and 90 °C and that of toluene between 60 and 90 °C. The measured data together with selected reference data are given in Table 1 for benzene and in Table 2 for toluene. Based on this data (the difference between the measured and reference data points), the standard uncertainty of the vapor pressure measurements presented here was found to be better than 0.3 kPa.

Table 1. Accuracy of vapor pressure values of benzene (boiling point 80.1 °C) measured using the ERAVAP analyzer

T, °C	P, kPa	P^1, kPa	ΔP^1, kPa	P^2, kPa	ΔP^2, kPa	P^3, kPa	ΔP^3, kPa	P^4, kPa	ΔP^4, kPa	P^5, kPa	ΔP^5, kPa
40.0	24.1	24.4	–0.3	24.4	–0.3	24.4	–0.3	24.4	–0.3	24.4	–0.3
50.0	36.2	36.2	0.0	36.2	0.0	36.2	0.0	36.2	0.0	36.2	0.0
60.0	52.3	52.2	0.1	52.2	0.1	52.2	0.1	52.2	0.1	52.2	0.1
70.0	73.4	73.4	0.0	73.5	–0.1	73.4	0.0	73.5	–0.1	73.4	0.0
80.0	100.9	101.0	–0.1	101.0	–0.1	101.0	–0.1	101.0	–0.1	101.0	–0.1
90.0	135.8	136.1	–0.3	136.1	–0.3	136.1	–0.3	136.1	–0.3	136.1	–0.3

Note: [1] is reference [42], [2] is reference [43], [3] is reference [44], [4] is reference [46], [5] is reference [47].

Table 2. Accuracy of vapor pressure values of toluene (boiling point 110.6 °C) measured using the ERAVAP analyzer

T, °C	*P*, kPa	P^1, kPa	ΔP^1, kPa	P^2, kPa	ΔP^2, kPa	P^3, kPa	ΔP^3, kPa	P^4, kPa	ΔP^4, kPa
60.0	18.6	18.5	0.1	18.5	0.1	18.5	0.1	18.5	0.1
70.0	27.4	27.2	0.2	27.2	0.2	27.2	0.2	27.2	0.2
80.0	39.1	38.8	0.3	38.8	0.3	38.8	0.3	38.8	0.3
90.0	54.1	54.2	–0.1	54.2	–0.1	54.2	–0.1	54.2	–0.1

Note: [1] is reference [42], [2] is reference [48], [3] is reference [44], [4] is reference [49].

Comparison of measured data with easy-to-use conventional oil vapor pressure correlations was performed using the root mean squared error (RMSE) and residual (a simple difference between predicted and measured values, r):

$$RMSE = \sqrt{\frac{\sum(\theta_p - \theta_m)^2}{n}}, \quad (1)$$

$$r = \theta_m - \theta_p, \quad (2)$$

where θ_p is the predicted value, θ_m is the measured value and n is the number of data points.

2.3. Determination of fraction properties

The characteristic properties of the fractions used in this study (density at 20 °C, refractive index at 20 ° C, average boiling point, K_W factor) are given in Table 3. The density at 20 °C was measured using a DMA 5000M density meter (Anton Paar GmbH, Graz, Austria). The instrument has a reproducibility of 0.00005 g/cm³. For gasoline samples, the standard uncertainty was found to be 0.00015 g/cm³. The refractive index at 20 °C was measured on an Abbemat HT refractometer (Anton Paar GmbH, Graz, Austria) at a wavelength of 589.592 nm. For gasoline samples, the standard uncertainty was found to be 0.0011. The average boiling point of narrow boiling range fractions was determined as the arithmetic mean of the lower and upper temperature limits of the fraction collected during rectification (provided that the fraction had a Gaussian boiling point distribution), with a measurement uncertainty of 1 °C. For fraction 4 alone, the average boiling point was not calculated because, due to an experimental error in collecting this fraction, its initial boiling point was higher than the final boiling point. The K_W factor, also called the Watson characterization factor or the Universal Oil Products Company (UOP) characterization factor, was calculated from measured density and average boiling point values according to the following equation:

Table 3. Properties of narrow boiling gasoline fractions

Fraction	T_{av}, °C	ρ, g/cm^3	*RI*	K_W
1	63	0.71033	1.4053	11.9
2	77	0.73005	1.4161	11.7
3	92	0.74776	1.4235	11.5
4		0.74978	1.4254	11.5*
5	89	0.74188	1.4210	11.6
6	99	0.76079	1.4299	11.5
7	108	0.78518	1.4420	11.2
8	115	0.76604	1.4314	11.5
9	119.5	0.76254	1.4298	11.6
10	123.5	0.77531	1.4359	11.4
11	130	0.79599	1.4466	11.2
12	137	0.80901	1.4524	11.1

Note: T_{av} – average boiling point, ρ – density at 20 °C, *RI* – refractive index at 20 °C, K_W – Watson characterization factor.
* Indicative K_w value, calculated using the normal boiling point calculated from the integrated Clausius-Clapeyron equation (integrated Clausius-Clapeyron equation constants are reported in Table 5).

$$K_w = \frac{\sqrt[3]{T_{av}}}{S}, \tag{3}$$

where T_{av} is the fraction's average boiling point, R, and S is the specific gravity at 60 °F. (However, in this study we used the density at 20 ° C, instead of 15.5 °C, to calculate specific gravity because the corresponding error was judged to be insignificant in our calculations). For fraction 4, the indicative value of K_w was calculated using the normal boiling point (estimated through the integrated Clausius-Clapeyron equation, Eq. (4)).

3. Results and discussion

3.1. Vapor pressure data

The experimental vapor pressure data for the twelve Kukersite oil shale retort oil narrow boiling range gasoline fractions is given in Table 4 and is shown graphically in Figure 1. The vapor pressures of all the fractions exhibited a linear trend on the ln(P) versus 1/T plot, and the R^2 correlation coefficient values were greater than 0.9995 for all the samples. Therefore, the integrated form of the Clausius-Clapeyron equation (Eq. (4)) was used to fit the

Table 4. Vapor pressure values (kPa) for the Kukersite oil shale derived gasoline fractions (Fr.) measured at different temperatures (*T*, °C)

T, °C	Fr. 1	Fr. 2	Fr. 3	Fr. 4	Fr. 5	Fr. 6	Fr. 7	Fr. 8	Fr. 9	Fr. 10	Fr. 11	Fr. 12
40.0	53.5	37.6	27.1	25.7	21.9							
50.0	75.7	53.5	39.7	36.9	32.1	22.5						
60.0	104.2	74.4	56.6	51.9	45.9	33.6	25.4					
70.0	140.8	101.3	77.8	71.3	64.4	47.2	36.7	30.1	23.8			
80.0	185.9	135.5	104.1	95.9	88.2	64.7	50.8	41.8	34.5	41	26.3	21.3
90.0	241.7	178.0	136.8	126.9	118.5	87.3	69	56.9	47.8	58	36.9	30.2
100.0	309.7	230.2	176.9	165.2	156.6	115.8	92.5	76.3	65.5	78.5	51.8	42.4
110.0	391.4	293.0	225.7	211.7	203.3	151.5	122.6	101.3	88.5	106.2	72.4	57.8
120.0	489	368.8	285.3	268.2	260.6	198.3	159.7	135.1	117.1	141.6	97.1	77.4

Table 5. Regression parameters A and B, heats of vaporizations (ΔH) and normal boiling points (T_b) for the Kukersite oil shale derived gasoline fractions studied

Fraction	A	B	ΔH, kJ/mol	T_b, °C
1	3398.5 ± 22.0	14.8 ± 0.1	28.3 ± 0.2	59.2
2	3513.1 ± 14.6	14.9 ± 0.0	29.2 ± 0.1	70.1
3	3601.9 ± 60.6	14.8 ± 0.2	29.9 ± 0.5	79.7
4	3607.3 ± 17.3	14.8 ± 0.0	30.0 ± 0.1	82.1
5	3812.2 ± 19.2	15.3 ± 0.1	31.7 ± 0.2	84.8
6	3906.6 ± 62.2	15.2 ± 0.2	32.5 ± 0.5	95.1
7	3995.7 ± 38.4	15.2 ± 0.1	33.2 ± 0.3	103.1
8	4032.0 ± 77.9	15.1 ± 0.2	33.5 ± 0.6	109.7
9	4286.4 ± 54.0	15.7 ± 0.1	35.6 ± 0.4	114.7
10	4283.5 ± 77.5	15.8 ± 0.2	35.6 ± 0.6	108.3
11	4563.6 ± 116.3	16.2 ± 0.3	37.9 ± 1.0	121.4
12	4486.9 ± 55.3	15.8 ± 0.1	37.3 ± 0.5	129.4

experimental data of the fractions as follows:

$$\ln P = -\frac{A}{T} + B = \frac{-\Delta H_{vap}}{RT} + B, \tag{4}$$

where P is the vapor pressure, kPa; ΔH_{vap} is the heat of vaporization, J mol^{-1}; T is the temperature, K; A and B are fitting constants and R is the ideal gas constant (8.314 J mol^{-1} K^{-1}). For each fraction the values of fitting constants A and B, together with the calculated heat of vaporization (from the fitting constant A) and atmospheric boiling point values (calculated at pressure 101.3 kPa) are given in Table 5.

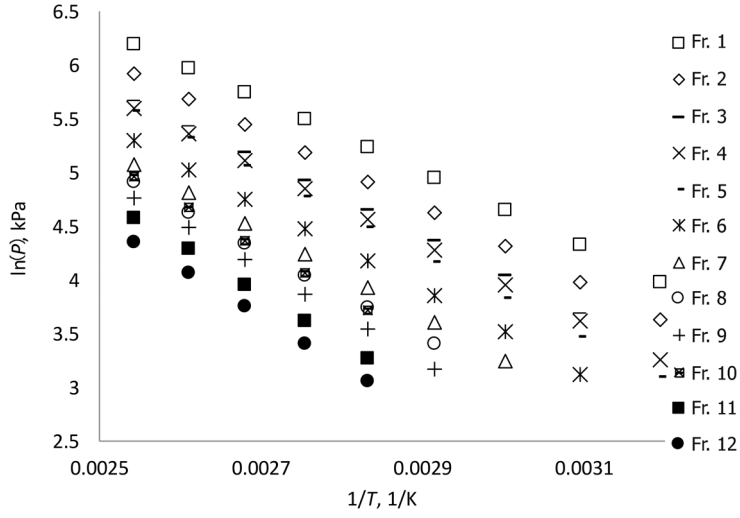

Fig. 1. Vapor pressures of Kukersite oil shale derived gasoline fractions on a 1/T vs ln(P) plot.

3.2. Evaluation of the applicability of prediction methods to oil shale gasoline

Various prediction methods, such as equations and graphs of varying degrees of complexity, have been developed to predict the vapor pressure of liquid fuels [5, 6]. In this study only easy-to-use methods, i.e. those based on conveniently measureable input parameters, were selected for evaluation. Correlations requiring critical temperature, critical pressure and acentric factor, i.e. parameters estimated by conventional oil-based empirical correlations, remained beyond consideration. The selected correlations were the following: a correlation from Van Nes and Van Westen [35], the Maxwell and Bonnell correlations [36, 37] and the modification to the Maxwell and Bonnell correlations presented by Tsonopoulos et al. [6] and Wilson et al. [38].

The correlation from Van Nes and Van Westen [35] is expressed by Equation (5) as follows:

$$log_{10}P_T = 3.2041\left(1 - 0.998 \cdot \frac{T_b - 41}{T - 41} \cdot \frac{1393 - T}{1393 - T_b}\right), \quad (5)$$

where P_T is the vapor pressure, bar, at temperature T, K, and T_b is the normal boiling point, K.

The Maxwell and Bonnell correlations [36, 37] are written as:

$$log_{10}P^{vap} = \frac{3000.538Q - 6.761560}{43Q - 0.987672} \text{ for Q} > 0.0022 \ (P^{vap} < 2 \text{ torr}), \quad (6)$$

$$log_{10}P^{vap} = \frac{2663.129Q - 5.994296}{95.76Q - 0.972546} \text{ for } 0.0013 \leq \text{Q} \leq 0.0022 \ (2 \text{ torr} \leq P^{vap} \leq 760 \text{ torr}), \quad (7)$$

$$log_{10}P^{vap} = \frac{2770.085Q - 6.412631}{36Q - 0.989679} \text{ for Q} < 0.0013 \ (P^{vap} > 760 \text{ torr}), \quad (8)$$

$$Q = \frac{\frac{T_b'}{T} - 0.00051606T_b'}{748.1 - 0.3861T_b'}, \quad (9)$$

$$T_b' = T_b - \Delta T_b, \quad (10)$$

$$\Delta T_b = 1.3889F(K_W - 12)log_{10}\frac{P^{vap}}{760}, \quad (11)$$

$$F = 0 \quad \text{if } T_b < 367\text{K if } T_b < 367\text{K}, \quad (12)$$

$$F = -3.2985 + 0.009T_b \text{ if } T_b \geq 367\text{K}, \quad (13)$$

where P^{vap} is the vapor pressure, Torr; T is the temperature at which the vapor pressure is to be calculated, K; T_b is the normal boiling point, K; T_b' is the normal boiling point corrected to the Watson characterization factor $K_W = 12$, K; F is the correction factor for the fractions with a K_W different than 12 (crude oils are classified as paraffinic with K_W between 11 and 12.9).

The modification to the Maxwell and Bonnell correlations presented by Tsonopoulos et al. [6] and Wilson et al. [38] gives equations which replace Equations (11)–(13):

$$\Delta T_b = F_1F_2F_3, \quad (14)$$

$$F_1 = \begin{cases} 0, & T_b \leq 366.5K \\ -1 + 0.009(T_b - 255.37), & T_b > 366.5K \end{cases}, \quad (15)$$

$$F_2 = (K_W - 12) - 0.01304(K_W - 12)^2, \tag{16}$$

$$F_3 = \begin{cases} 1.47422 log_{10} P^{vap}, & P^{vap} \leq 1atm \\ 1.47422 log_{10} P^{vap} + 1.190833 (log_{10} P^{vap})^2, & P^{vap} > 1atm \end{cases}, \tag{17}$$

where P^{vap} is in the units of atm.

The RMSEs (3.4, 2.9 and 2.9 kPa, respectively) of the predicted vapor pressure values for each correlation show that, overall, the three selected correlations performed similarly, although the Maxwell and Bonnell correlations were slightly more accurate than the Van Nes and Van Westen correlation. Also the trend in the residuals was similar for all the correlations. The residuals of each point of the Maxwell and Bonnell correlations and the Van Nes and Van Westen correlation are shown in Figure 2 (individual fractions are not distinguished). The corresponding relative deviation of the predicted values was typically less than 5%.

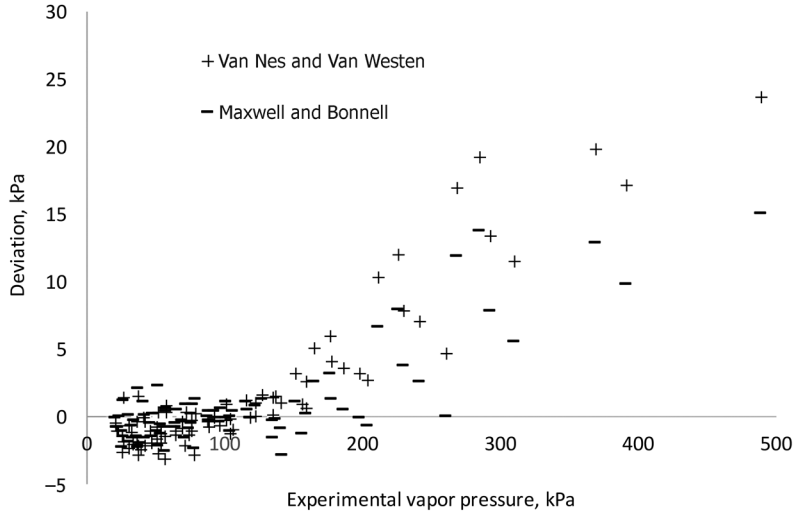

Fig. 2. Deviation of predicted vapor pressure values from the experimental values (given as predicted value minus measured value).

Due to the fixed temperature range of the measuring apparatus, 273–393 K, and the different volatilities of the fractions, their measured vapor pressure ranges varied significantly, the vapor pressure of fraction 1 was measured between 53.5 and 489 kPa, and that of fraction 12 between 21.3 and 77.4 kPa. Therefore, to better illustrate the performance of easy-to-use conventional

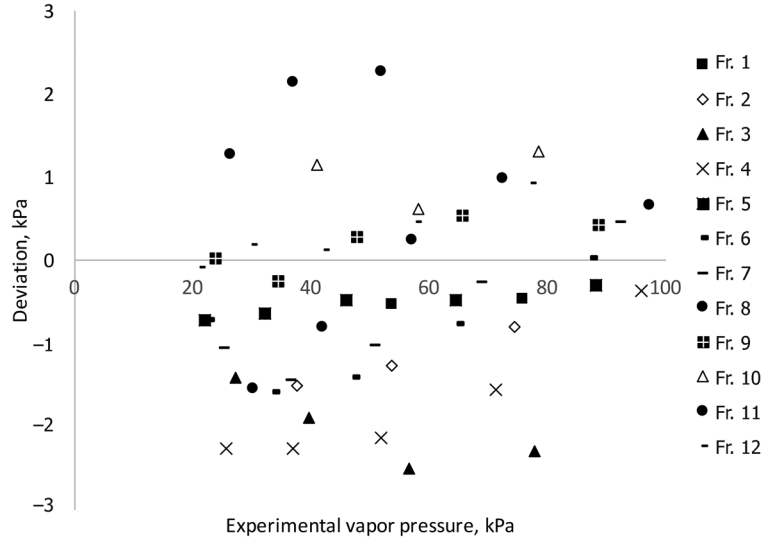

Fig. 3. Deviation of vapor pressure values predicted by the Maxwell and Bonnell correlations, from the experimental values, illustrated for all fractions at pressures up to 100 kPa.

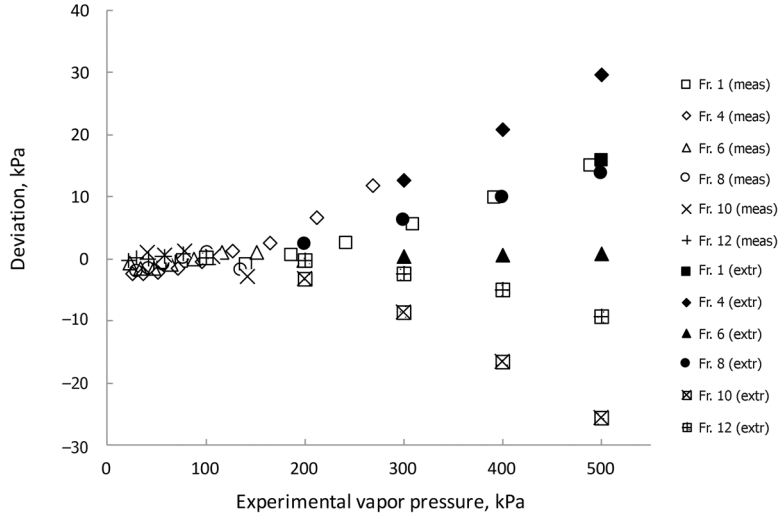

Fig. 4. Deviation of vapor pressures predicted by the Maxwell and Bonnell equation from the experimental values, illustrated for selected fractions at pressures up to 500 kPa. Experimental data-based residuals are shown as open points and extrapolated data-based residuals as solid points. (Abbreviations: meas – measured, extr – extrapolated.)

oil equations, the Maxwell and Bonnell correlations-based comparison is presented somewhat differently in Figures 3 and 4. Figure 3 shows the residuals, distinguishing each fraction specifically, up to a pressure of 100 kPa. It can be seen from Figure 3 that the residues vary quite randomly by fraction, the behavior of fractions exhibiting random variation around the average deviation trend. At the same time, the predicted vapor pressure values have a deviation of ± 2.5 kPa, while the relative deviation at 50 kPa is less than 5%. Some explanations for this, more like random variation, can be derived from the data in Table 3. Table 3, which contains characteristic data, shows that as the fraction number increases, there is no strictly monotonic increase in density or refractive index; rather, slight local minima and maxima can be seen in the generally increasing behavior with an increase in the initial boiling point. Assuming that the uncertainty associated with distillation is not so significant, this may indicate that the rectification results in the dominance of different classes of compounds among the boiling regions of the fractions. Figure 4 shows residuals for six selected fractions up to 500 kPa, displaying both experimental data-based residuals (open points) and extrapolated data-based residues (solid points). The extrapolation beyond the measurement region is done here for illustrative purposes only. Again, the residuals vary quite randomly by fraction and the corresponding relative deviations of the predicted values fall below 5%.

In summary, the easy-to-use vapor pressure correlations, which were evaluated in this study, can be used to get reasonable estimates of the vapor pressure for these types of shale oil gasoline fractions and a choice between them could be merely a matter of convenience.

4. Conclusions

This article presented vapor pressure data for the narrow boiling fractions (or pseudocomponents) prepared by rectification from a wide technical gasoline fraction, which in turn was produced from Kukersite oil shale by using solid heat carrier retorting technology. Basic characteristics information (specific gravity, refractive index, average boiling point) was also measured for these fractions. It was found that the three examined easy-to-use correlations (which were based on conveniently measureable input parameters, either atmospheric boiling point or atmospheric boiling point and the characterization K_W factor calculable on the basis of density and average boiling point) provided reasonable estimates of the vapor pressure of the gasoline fractions studied, while the choice between them could be merely a matter of convenience. In general, the performance of the different correlations was similar, although the Maxwell and Bonnell correlations were a little more accurate than the Van Nes and Van Westen correlation. The relative deviation of the predicted values was below 5% on average.

Acknowledgement

Support for the research was provided by the National R&D program "Energy" under project AR10129 "Examination of the Thermodynamic Properties of Relevance to the Future of the Oil Shale Industry" (P.I. Prof Vahur Oja).

REFERENCES

1. Riazi, M. R., Al-Enezi, G. A. Modelling of the rate of oil spill disappearance from seawater for Kuwaiti crude and its products. *Chem. Eng. J*., 1999, **73**(2), 161–172.
2. Raj, P. K. A flammability (risk) index for use in transportation of flammable liquids. *J. Loss Prevent. Proc*., 2016, **44**, 755–763.
3. Pichler, H., Lutz, J. Why crude oil vapor pressure should be tested prior to rail transport. *Adv. Petrol. Explor. Dev.*, 2014, **7**(2), 58–63.
4. Andersen, V. F., Anderson, J. E., Wallington, T. J., Mueller, S. A., Nielsen, O. J. Vapor pressures of alcohol−gasoline blends. *Energ. Fuel.*, 2010, **24**(6), 3647–3654.
5. Riazi, M. R. *Characterization and Properties of Petroleum Fractions*. ASTM International, 2005.
6. Tsonopoulos, C., Heidman, J. L., Hwang, S.-C. *Thermodynamic and Transport Properties of Coal Liquids*. Wiley, 1986.
7. Nji, G. N., Svrcek, W. Y., Yarranton, H. W., Satyro, M. A. Characterization of heavy oils and bitumens. 1. Vapor pressure and critical constants prediction methods for heavy hydrocarbons. *Energ. Fuel.*, 2008, **22**(1), 455–462.
8. Oja, V., Suuberg, E. M. Oil shale processing, chemistry and technology. In: *Encyclopedia of Sustainability Science and Technology* (Meyers, R. A., ed.). Springer, 2012, 7457−7491.
9. Lee, S. *Oil Shale Technology*. CRC Press, 1990.
10. Ge, X., Wang, S., Jiang, X. Catalytic effects of shale ash with different particle sizes on characteristics of gas evolution from retorting oil shale. *J. Therm. Anal. Calorim*., 2019, **138**, 1527−1540.
11. Yu, X., Luo, Z., Li, H., Zhang, J., Gan, D. The diffusion and separation of the oil shale in the compound dry beneficiation bed. *Powder Technol.*, 2019, **355**, 72−82.
12. Qian, J. L., Yin, L., Wang, J. Q., Li, S. Y., Han, F., He, Y. G. *Oil Shale – Petroleum Alternative*. China Petrochemical Press, Beijing, 2010.
13. Urov, K., Sumberg, A. Characteristics of oil shales and shale-like rocks of known deposits and outcrops. Monograph. *Oil Shale*, 1999, **16**(3S), 1−64.
14. Akalin, E., Kim, Y. M., Alper, K., Oja, V., Tekin, K., Durukan, I., Siddiqui, M. Z., Karagöz, S. Co-hydrothermal liquefaction of lignocellulosic biomass with Kukersite oil shale. *Energ. Fuel.*, 2019, **33**(8), 7424−7435.

15. Oja, V. Examination of molecular weight distributions of primary pyrolysis oils from three different oil shales via direct pyrolysis Field Ionization Spectrometry. *Fuel*, 2015, **159**, 759−765.
16. Siitsman, C., Oja, V. Application of a DSC based vapor pressure method for examining the extent of ideality in associating binary mixtures with narrow boiling range oil cuts as a mixture component. *Thermochim. Acta*, 2016, **637**, 24−30.
17. Akash, B. A., Characterization of shale oil as compared to crude oil and some refined petroleum products. *Energ. Source.*, 2003, **25**(12), 1171–1182.
18. Kollerov, D. K. *Physicochemical Properties of Oil Shale and Coal Liquids*. Moscow, 1951 (in Russian).
19. Oja, V., Rooleht, R., Baird, Z. S. Physical and thermodynamic properties of kukersite pyrolysis shale oil: literature review. *Oil Shale*, 2016, **33**(2), 184–197.
20. Oja, V. Is it time to improve the status of oil shale science? *Oil Shale*, 2007, **24**(2), 97−100.
21. Johannes, I., Luik, H., Bojesen-Koefoed, J. A., Tiikma, L., Vink, N., Luik, L. Effect of organic matter content and type of mineral matter on the oil yield from oil shales. *Oil Shale*, 2012, **29**(3), 206–221.
22. Baird, Z. S., Uusi-Kyyny, P., Järvik, O., Oja, V., Alopaeus, V. Temperature and pressure dependence of a shale oil and derived thermodynamic properties. *Ind. Eng. Chem. Res*., 2018, **57**(14), 5128–5135.
23. Baird, Z. S., Uusi-Kyyny, P., Oja, V., Alopaeus, V. Hydrogen solubility of shale oil containing polar phenolic compounds. *Ind. Eng. Chem. Res*., 2017, **56**(30), 8738–8747.
24. Rannaveski, R., Listak, M., Oja, V. ASTM D86 distillation in the context of average boiling points as thermodynamic property of narrow boiling range oil fractions. *Oil Shale*, 2018, **35**(3), 254–264.
25. Siitsman, C., Oja, V. Extension of the DSC method to measuring vapor pressures of narrow boiling range oil cuts. *Thermochim. Acta*, 2015, **622**, 31–37.
26. Siitsman, C., Kamenev, I., Oja, V. Vapor pressure data of nicotine, anabasine and cotinine using differential scanning calorimetry. *Thermochim. Acta*, 2014, **595**, 35–42.
27. Astra, H.-L., Oja, V. Vapour pressure data for 2-n-propylresorcinol, 4-ethylresorcinol and 4-hexylresorcinol near their normal boiling points measured by differential scanning calorimetry. *J. Chem. Thermodyn*., 2019, **134**, 119–126.
28. Gray, J. A., Holder, G. D., Brady, C. J., Cunningham, J. R., Freeman, J. R., Wilson, G. M. Thermophysical properties of coal liquids. 3. Vapor pressure and heat of vaporization of narrow boiling coal liquid fractions. *Ind. Eng. Chem. Proc. Des. Dev*., 1985, **24**(1), 97–107.
29. Oja, V., Suuberg, E. M. Development of a nonisothermal Knudsen effusion method and application to PAH and cellulose tar vapor pressure measurement. *Anal. Chem*., 1997, **69**(22), 4619–4626.
30. Castellanos-Diaz, O., Schoeggl, F. F., Yarranton, H. W., Satyro, M. A. Measurement of heavy oil and bitumen vapor pressure for fluid characterization. *Ind. Eng. Chem. Res*., 2013, **52**(8), 3027–3035.

31. Oja, V., Suuberg, E. M. Measurements of the vapor pressures of coal tars using the nonisothermal Knudsen effusion method. *Energ. Fuel.*, 1998, **12**(6), 1313–1321.
32. Spencer, W. F., Cliath, M. M. Measurement of pesticide vapor pressures. In: *Residue Reviews* (Gunther, F. A., Gunther, J. D., eds.), Springer, New York, 1983, 57–71.
33. Rannaveski, R., Oja, V. A new thermogravimetric application for determination of vapour pressure curve corresponding to average boiling points of oil fractions with narrow boiling ranges. *Thermochim. Acta*, 2020, **683**, Article 178468.
34. ASTM D6378-10. *Standard Test Method for Determination of Vapor Pressure (VPX) of Petroleum Products, Hydrocarbons, and Hydrocarbon-Oxygenate Mixtures (Triple Expansion Method*). ASTM International, West Conshohocken, PA, USA, 2016.
35. Van Nes, K., Van Westen, H. A. *Aspects of the Constitution of Mineral Oils*. Elsevier Publishing Company, 1951.
36. Maxwell, J. B., Bonnell, L. S. *Vapor Pressure Charts for Petroleum Hydrocarbons*. Esso Research and Engineering Company, 1955.
37. Maxwell, J. B., Bonnell, L. S. Derivation and precision of a new vapor pressure correlation for petroleum hydrocarbons. *Ind. Eng. Chem*., 1957, **49**(7), 1187–1196.
38. Wilson, G. M., Johnston, R. H., Hwang, S. C., Tsonopoulos, C. Volatility of coal liquids at high temperatures and pressures. *Ind. Eng. Chem. Proc. Des. Dev*., 1981, **20**(1), 94–104.
39. Golubev, N. Solid oil shale heat carrier technology for oil shale retorting. *Oil Shale*, 2003, **20**(3S), 324–332.
40. Elenurm, A., Oja, V., Tali, E., Tearo, E., Yanchilin, A. Thermal processing of dictyonema argillite and kukersite oil shale: Transformation and distribution of sulfur compounds in pilot-scale Galoter process. *Oil Shale*, 2008, **25**(3), 328−334.
41. ASTM D2892-15. *Standard Test Method for Distillation of Crude Petroleum (15-Theoretical Plate Column*). ASTM International, West Conshohocken, PA, 2015.
42. Dreisbach, R. R. *Physical Properties of Chemical Compounds*. Advances in Chemistry Series, **15**, Am. Chem. Soc., Washington, D. C, 1955.
43. Boublik, T., Fried, V., Hala, E. *The Vapor Pressure of Pure Substances*, 2nd revised Edition. Elsevier, Amsterdam, The Netherlands, 1984.
44. Zwolinski, B. J., Wilhoit, R. C. *Handbook of Vapor Pressures and Heats of Vaporization of Hydrocarbons and Related Compounds*. API-44, TRC Publication No. 101, Texas A&M University, College Station, TX, 1971.
45. Stephenson, R. M., Malanowski, S. *Handbook of the Thermodynamics of Organic Compounds*. Elsevier, New York, 1987.
46. Ambrose, D., Ewing, M. B., Ghiassee, N. B., Sanchez Ochoa, J. S. The ebulliometric method of vapour-pressure measurement: vapour pressures of benzene, hexafluorobenzene, and naphthalene. *J. Chem. Thermodyn*., 1990, **22**(6), 589−605.

47. Connolly, J. F., Kandalic, G. A. Saturation properties and liquid compressibilities for benzene and n-octane. *J. Chem. Eng. Data*, 1962, **7**(1),137−139.
48. Dean, J. A., Ed. *Lange's Handbook of Chemistry*. 14th Edition, McGraw-Hill, New York, 1992.
49. Willingham, C. B., Taylor, W. J., Pignocco, J. M., Rossini, F. D. Vapor pressures and boiling points of some paraffin, alkylcyclopentane, alkylcyclohexane, and alkylbenzene hydrocarbons. *J. Res. Natl. Bur. Stand*., 1945, **35**, 219−244.

Received January 06, 2020